LA-UR- 94-3744

Conf-940629l--1

TITLE: SECOND GENERATION INTERFEROMETRY MEASUREMENTS AT CERN

AUTHOR(S): John P. Sullivan, P-25

SUBMITTED TO: Proceedings of the "5th Conference on the Intersections of Particle and Nuclear Physics", Tampa, FL, June 1-6, 1994

DISCLAIMER

SECOND GENERATION INTERFEROMETRY MEASUREMENTS AT CERN

J. P. Sullivan
Los Alamos National Laboratory
Los Alamos, NM 87545

Abstract

Source size parameters measured via two-particle interferometry in experiment NA44 for 200 GeV/nucleon S+Pb collisions are compared to calculations using the RQMD event generator. Reasonable agreement is found in most cases. The event generator is then used to compare the "true" size of the particle-emitting source to the measured size parameters and to discuss the difficulties in defining the "true" source size.

Introduction

The first experiments with high energy heavy ion beams at CERN (e.g. NA35[1] and Helios[2]) made measurements of many particles types over a wide kinematic region. NA44 is one of the second generation of heavy-ion experiments at CERN and was designed to pursue some of the more interesting results from the first generation — the large source sizes observed via two-particle interferometry[1] and the excess of low p_T pions[1, 2]. Towards these ends, NA44 was optimized for the study of single particle spectra and two-particle particle spectra near mid-rapidity for transverse momenta below $\approx$ 1 GeV/c. This paper will concentrate on the source size parameters determined from fits to two-particle correlation functions. The relationship between these size parameters and the true size of the source which emitted the particles will be examined using the RQMD event generator[3, 4].

Experimental Results

The NA44 Focusing Spectrometer[5, 6, 7], which uses two dipole magnets and three quadrupoles, covers a momentum range of $\pm 20\%$ around its central momentum setting. For the data shown here, the central momentum settings are 4 GeV/c (lab) for pions and 6 GeV/c for kaons. The two spectrometer angle settings used for π^+ , 44 mrad and 122 mrad, are referred to as low p_T ($< p_T > \approx 150$ MeV/c) and high p_T ($< p_T > \approx 450$ MeV/c), respectively. The tracking and time-of-flight uses three scintillator hodoscopes whose time resolution is $\approx$ 100 ps, with a Cherenkov beam counter[8] for the time-of-flight start ($\sigma \approx 35$ ps).

The NA44 data have been analyzed in terms of three components[9, 10] of the two-particle momentum difference ($\vec{q} = \vec{p_1} - \vec{p_2}$). The data are analyzed in the frame in which the z-component of the pair momentum ($p_{z1} + p_{z2}$) is zero (the longitudinal center of mass system, or "LCMS"). The momentum difference is resolved into a component

(q_{beam}) parallel to the beam direction and a component perpendicular to the beam direction. The perpendicular component is further resolved into q_{out} parallel to the sum of the pair momentum and q_{side}, which is perpendicular to the sum and to the beam. Three corresponding source size parameters (R_{beam}, R_{out}, R_{side}) are simultaneously fit to measured 3D correlation functions from two different spectrometer settings. The "horizontal" focus spectrometer setting optimizes the acceptance for R_{out}, while the "vertical" focus spectrometer setting is for R_{side}. The resolution in q_{out} and q_{beam} is $\approx$15 MeV/c and in q_{side} is $\approx$30 MeV/c.

Discussion

Fig. 1 compares size parameters from NA44[5, 6, 7] to size parameters calculated[11] by using the RQMD event generator[3, 4] to generate the single particle emission probability distribution at the point of each particle's last interaction. The two-particle correlation function is calculated from the single particle distribution using a Wigner function formalism[12, 13]. In fig. 1, the calculations for low p_T π^+ agree with the NA44 results for two of three size components, but the RQMD result is larger (by 3.4σ) than the NA44 result for R_{beam}. The RQMD result also agrees with the NA44 high p_T result for two of three size parameters, put the RQMD value of R_{out} is significantly larger than the NA44 result. For K^+, the NA44 and RQMD results are in good agreement.

In the simplest view of boson interferometry, there is a static source with no correlations between the momentum and position of a particle. These assumptions lead from a source position distribution of the form

$$\rho(r) \propto \exp(-\frac{r^2}{2R_{gauss}^2}), \qquad (1)$$

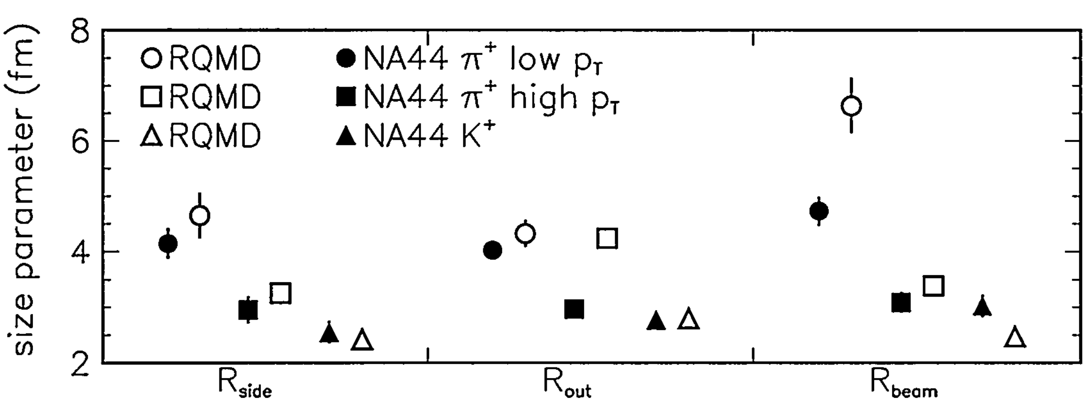

Figure 1: The size parameters, for 200 GeV/nucleon S+Pb, based on fits to 3 dimensional correlation functions, for low p_T π^+ (solid circles), high p_T π^+ (solid squares), and for K^+ pairs (solid triangles) from NA44. The corresponding fit parameters from the correlation functions calculated from RQMD are shown as open symbols.

where r is the position of a particle's last interaction and R_{gauss} is a size parameter, to a correlation function of the form

$$C_2(q) = 1 + \exp(-q^2 R_{gauss}^2), \tag{2}$$

where q is the two-particle momentum difference. When there are correlations between r and the particle's momentum, the size parameter measured by interferometry (eq. 2) is generally different than the "true" size of the source (R_{gauss} in eq. 1). Studies with event generators[11, 14, 15, 16] and the kinematics of particle generation[17] both lead to the belief that such correlations do exist in high energy heavy ion collisions. Using an event generator, we can try to relate measured radius parameters, which come from a fit to a correlation function, to the "true" source size. One complication in the process is that, because the source position distribution is not a gaussian as in eq. 1, the "true" size does not always have an obvious definition.

Ideally the source "size" could be defined with one or two numbers, such as the transverse and longitudinal widths of the source position distribution, which would completely specify the source distribution. Unfortunately, for heavy ion collisions around

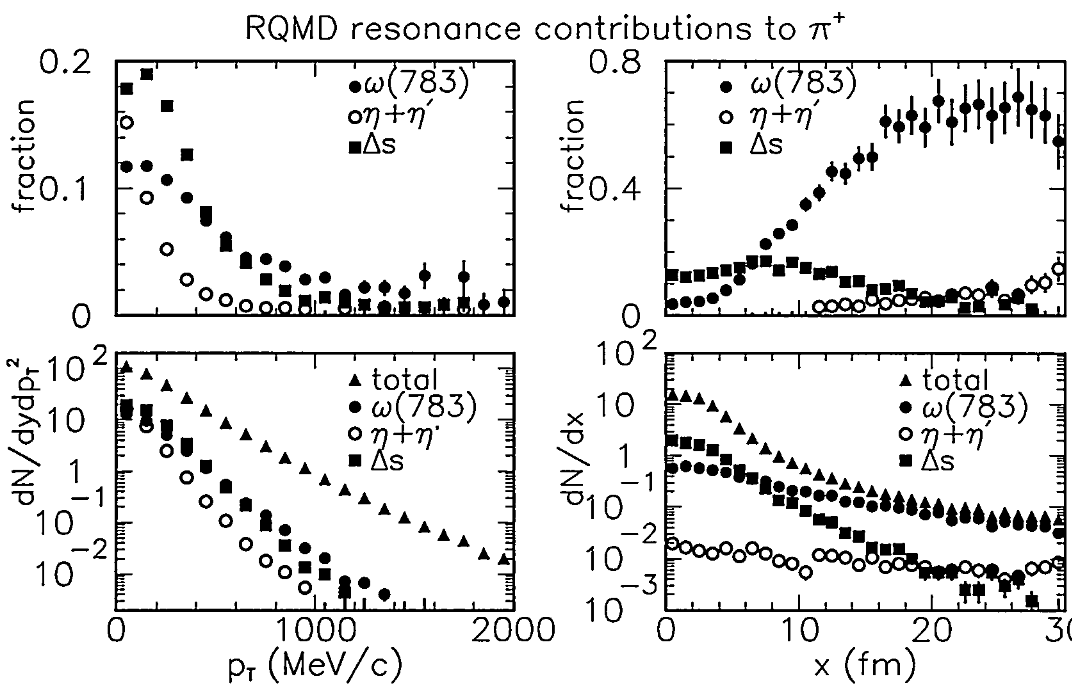

Figure 2: In 200 GeV/nucleon RQMD events, the fraction of all π^+ coming the decay of various resonances vs. p_T (top left) and x (top right), plus the p_T (bottom left) and x (bottom right) distributions from each of these sources along with the total p_T and x distributions. Only pions with $2 < y < 4$ are shown. X is one of the transverse coordinates.

200 GeV/nucleon, the large fraction of pions which come from resonances such as the $\omega(783)$, η, and η' complicate such a definition. The RQMD event generator can be used to study this question more quantitatively. Source position and momentum distributions for π^+'s from 200 GeV/nucleon S+Pb RQMD events are shown in fig. 2. The position distributions show the transverse position (x) at the point of the particle's last interaction. The momentum distributions are based on the particle momentum at the detector. Ideally, the x distribution (bottom right of fig. 2) could be fit with a gaussian of the form shown in eq. 1. Such a fit gives a reasonable description of the π^+ transverse position distribution from 0 to about 6-8 fm. However there is a long, approximately exponential, tail to the distribution which extends to larger x values and comes mainly from decays of the $\omega(783)$. To demonstrate this, the right side of fig. 2 shows x distributions for all pions in the range $2 < y < 4$ and for those pions coming from various resonance decays. For x $\approx$ 23 fm, corresponding to the $\omega(783)$ lifetime, pions from $\omega(783)$ decay become the dominant contribution. For x large compared to the $\omega(783)$ lifetime, the dominant components become first pions from η' decay, then the η decay. Another way to define the "size" is to find the RMS width of the source distribution. Because the η and η' components extend to extremely large sizes, some cutoff must be applied. The detector's finite momentum resolution makes the NA44 ex-

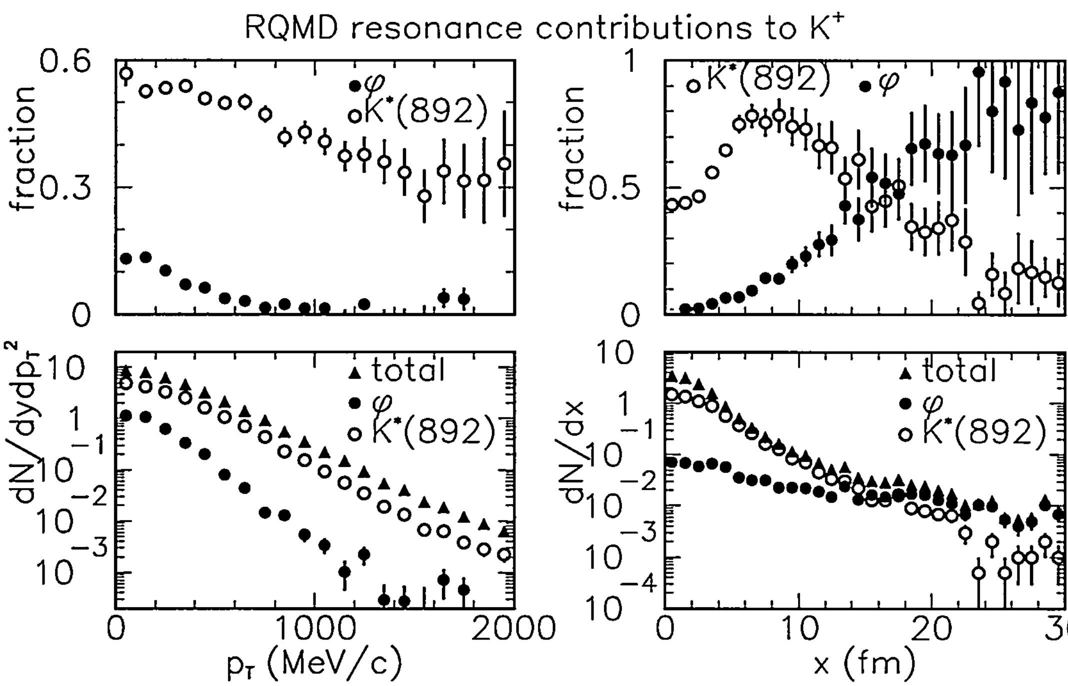

Figure 3: In 200 GeV/nucleon RQMD events, the fraction of all K^+ coming the decay of various resonances vs. p_T (top left) and x (top right), plus the p_T (bottom left) and x (bottom right) distributions from each of these sources along with the total p_T and x distributions. Only K^+ with $2 < y < 4$ are shown. X is one of the transverse coordinates.

periment insensitive to structure in the correlation function finer than ≈10 MeV/c, so this cutoff is placed at 20 fm≈ $\hbar c$/10 MeV/c). "Sizes" based on both of these definitions are given in table 1. The differences between the RMS and R_{gauss} values in table 1 are a measure of the resonance contributions — RMS values larger than R_{gauss} come from the long tails on the position distributions. The left side of fig. 2 shows the resonance contributions to the π^+ spectrum as a function of p_T. These resonance contributions can be substantially reduced by measuring at higher p_T.

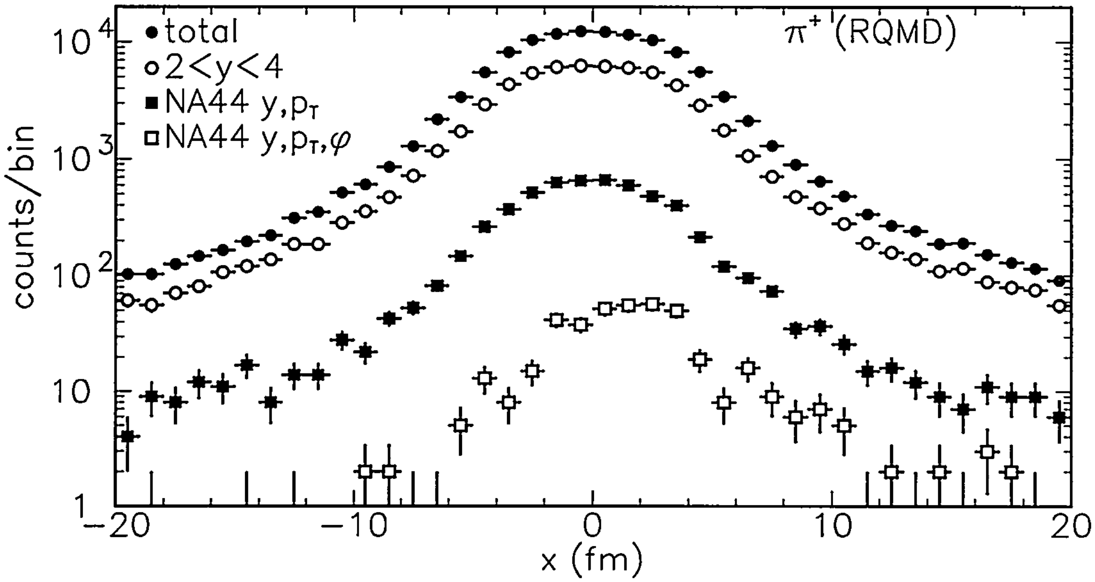

Figure 4: The position distribution in "x" (one of the transverse coordinates) for π^+ in 200 GeV/nucleon RQMD events. The distributions for all π^+ (solid circles), for the lab rapidity range $2 < y < 4$ (open circles), for the y and p_T range covered by the NA44 spectrometer in the low p_T setting (solid squares), and for π^+ in the y, p_T, and ϕ range of the NA44 spectrometer (open squares) are shown.

Fig. 3 is similar to fig. 2, except it shows the fractions and overall distributions of K^+ coming from the K^* and ϕ resonances as a function of p_T and x. A large fraction of all K^+ come from K^* decay, with the ϕ becoming more important at x ≈ 16 fm. The K^* lifetime is around 4 fm/c, which can contribute to the "size" measured by interferometry. However, according to RQMD, the slope of the p_T spectrum of K^+ from K^* decay is similar to the overall slope. Therefore the K^* contribution can not be easily eliminated by measuring at higher p_T. On the other hand, the ϕ contribution can be largely eliminated by measuring above 800 MeV/c.

The π^+ transverse position distributions, with various acceptance cuts, shown in fig. 4 further illustrate the difficulties in defining a "size" from the position distribution. First, the distribution for all π^+ with no acceptance cuts is shown. Below that, the distribution for π^+ in the range $2 < y < 4$ is shown — this cut reduces the total number of pions by a factor of ≈ 2 without changing the shape significantly. Fig. 4 also shows

Acceptance definition	Particle type	Mean (fm)	RMS (fm)	$< x >$ (fm)	R_{gauss} (fm)
no cuts	π^+	0.01±.01	4.37	0.01±.01	3.64±.01
$2 < y < 4$	π^+	-0.01±.02	4.48	-0.02±.02	3.67±.01
NA44 low p_T, y, p_T	π^+	-0.02±.06	4.41	-0.05±.05	3.36±.04
NA44 low p_T, y, p_T, ϕ	π^+	1.79±.20	4.34	1.24±.15	2.75±.18
NA44 high p_T, y, p_T	π^+	-0.09±.13	4.67	-0.09±.11	3.74±.09
NA44 high p_T, y, p_T, ϕ	π^+	3.64±.49	2.62	2.81±.25	1.12±.28
no cuts	K^+	0.02±.01	3.84	0.01±.01	2.90±.01
$2 < y < 4$	K^+	0.01±.02	3.98	0.02±.02	2.95±.02
NA44 y, p_T	K^+	0.04±.06	3.89	0.08±.05	2.87±.04
NA44 y, p_T, ϕ	K^+	1.77±.20	3.84	1.23±.16	2.57±.14

Table 1: For various acceptance cuts, the mean value and RMS deviations from the mean value of the transverse position along with the $< x >$ and R_{gauss} from fits of eq. 1 to the same distributions. RMS values are based on the range $-20 < x < 20$ fm only. Based on 200 GeV/nucleon RQMD events.

the distribution for all π^+ in the y and p_T range covered by the NA44 spectrometer at its low p_T setting. This cut, which neglects the NA44 spectrometer's azimuthal acceptance, also has little effect on the shape while reducing the overall number of counts by a factor of ≈ 5. Finally, when the azimuthal acceptance of the NA44 spectrometer is added to the y and p_T cuts, the distribution gets about 25% narrower, moves toward positive "x", and becomes asymmetric. The total number of counts drops by another factor of ≈ 10. In the coordinate system used, the NA44 spectrometer has an acceptance which is centered at positive p_x, covering only a very narrow range of $|p_y| < 20$ MeV/c. The result is that particles which enter the spectrometer are more likely to come from the side of the source closest to the spectrometer. This shift in x has been seen in earlier studies[15].

Table 1 shows the effects of the different acceptance cuts on the transverse position distributions for low p_T π^+ more quantitatively than fig. 4. The effects of the high p_T π^+ acceptance on the source distribution are also summarized in table 1. As for the low p_T setting, when the y, p_T, and azimuthal acceptance cuts are included, the x distribution shifts towards positive x (towards the detector) – but the shift is larger for the high p_T setting and the resulting distribution is narrower. For this choice of coordinate systems, the width in x is reflected mainly in the R_{out} size parameter. The measured R_{out} is smaller than the RQMD value of R_{out} at the high p_T spectrometer setting. This suggests that the observed transverse expansion could be faster than the expansion in RQMD — but this conclusion needs further study to confirm it. Qualitatively, this type of correlation between the position and momentum of the particle is expected for a system undergoing a transverse expansion. Table 1 also summarizes the effect of the different acceptance cuts on the width of the K^+ transverse position distribution. The effects of the acceptance on the K^+ and π^+ distributions are similar.

Conclusions

Source size parameters calculated from RQMD are in reasonable agreement with the results from NA44. If RQMD is then used to attempt to relate the source size parameters with the "true" source size, we see that the "true" source size is difficult to define with a single number. The widths of the RQMD source distributions for particles within the spectrometer's acceptance are smaller than the widths of the distributions without acceptance cuts and the center of the source distribution is shifted to the side closest to the detector. This behavior is consistent with expectations for a transversely expanding source. An expanding source helps explain why R_{out} is not larger than R_{side}, as would be expected for a static source[9, 10].

REFERENCES

1. P. Seyboth *et al.*, Nucl. Phys. A**544**, 293c (1992).
2. T. Åkesson *et al.*, Phys. Lett. B**214**, 25 (1988); T. Åkesson *et al.*, Z. Phys. C**46**, 361 (1990); T. Åkesson *et al.*, Z. Phys. C**46**, 369 (1990).
3. H. Sorge, H. Stöcker and W. Greiner, Nucl Phys. **A498**, 567c (1989); H. Sorge *et al.* Z. Phys. C**47**, 629 (1990).
4. H. Sorge *et al.* Phys. Lett. B**289**, 6 (1992).
5. H. Becker *et al.*, Phys. Lett. B**302**, 510 (1993).
6. H. Bøggild *et al.*, CERN-PPE/(94-75) (1994), in press, Z. Phys.
7. H. Becker *et al.*, submitted to Phys. Rev. Lett. (1994).
8. N. Maeda *et al*, Nucl. Inst. Meth. **A346**, 132 (1994).
9. S. Pratt, Phys. Rev. D**33**, 1314 (1986).
10. G. Bertsch, M. Gong, M. Tohyama, Phys. Rev. C**37**, 1896 (1988).
11. J. P. Sullivan *et al.*, Phys. Rev. Lett. **70**, 3000 (1993).
12. T. Csörgo *et al.*, Phys. Lett. B**241**, 301 (1990).
13. S. Pratt, T. Csörgo, J Zimányi, Phys.Rev C**42**, 2646 (1990).
14. Nu Xu, Nucl. Phys. A**566**, 585c (1994).
15. O. Vossnack, Nucl. Phys. A**566**, 535c (1994).
16. G. Roland, Nucl. Phys. A**566**, 527c (1994).
17. S. Padula, M. Gyulassy, Nucl. Phys. B**339**, 378 (1990).